



SEISMIC RISK ASSESSMENT OF CONVENTIONAL MASONRY CONSTRUCTION IN CANADA

Saeid MOJIRI

Former Graduate Student, Department of Civil Engineering, McMaster University, Canada
mojiris@mcmaster.ca

Wael W. EL-DAKHAKHNI

Martini, Mascarin and George Chair in Masonry Design, Co-Director, Centre for Effective Design of Structures, Department of Civil Engineering, McMaster University, Canada
eldak@macmaster.ca

Michael J. TAIT

Joe NG/JNE Consulting Chair in Design, Construction and Management in Infrastructure Renewal, Co-Director, Centre for Effective Design of Structures, Department of Civil Engineering, McMaster University, Canada
taitm@mcmaster.ca

ABSTRACT: With the North American seismic codes moving toward adopting performance-based seismic design approaches, there is a need to develop seismic probabilistic risk assessment (PRA) tools for different construction systems, including reinforced masonry (RM). This study first summarizes the test and analysis results of a series of concrete block walls with design parameters that categorize them as *conventional* (non-seismic) *construction* based on the National Building Code of Canada (2010). In general, the walls experienced minimal damage under low amplitude shaking corresponding to frequent minor earthquake events, incurred repairable damage for higher level tests, and maintained their integrity for the highest level tests corresponding to the highest seismicity zones in Canada. The paper then focuses on the characteristics of a simplified analytical model that is used to simulate the seismic response of the tested RM shear walls. The model is then used for the development of fragility curves, as an essential component of the PRA framework. The wall seismic demand levels are determined through a probabilistic approach by performing a series of inelastic response history analyses. In general, the results indicate that the RM conventional construction category evaluated within this study would experience an acceptable seismic performance, associated with moderate lateral wall top-roof drifts, and pose low levels of seismic risk even when subjected to ground motion records representing some of the highest seismic regions in eastern and western Canada.

1. Introduction

Fragility curves give information pertaining to the probability of a structure exceeding a certain limit state (associated with a certain damage level) if subjected to an earthquake with certain intensity. Fragility curves play an important role in seismic probabilistic risk assessment (PRA) and probabilistic performance-based seismic design and analysis of structures (ATC, 2012). With the computational advances and the availability of more reliable and powerful software tools, generation of fragility curves using probabilistic seismic demand analyses, based on nonlinear response history analysis (NRHA) of structures, has been becoming more common (Shome, 1999; Nielson, 2005). However, development of these analytical fragility curves is dependant on the availability of simple yet accurate corresponding analysis tools as well as the availability of realistic information on the characteristics and nature of seismic response of structures. The latter can be achieved by component/system level experimental testing of seismic force resisting systems (SFRS) using shake table facilities (ATC, 2007).

Masonry buildings constitute a major portion of urban construction in North America. The SFRS in these buildings is typically shear walls (Paulay and Priestley, 1992; Drysdale and Hamid, 2005). There has been an extensive number of research studies focusing on evaluating the seismic response of masonry construction when used with steel reinforcement. It has been shown that the general response and energy dissipation mechanisms of reinforced masonry (RM) walls can be very similar to reinforced concrete (RC) shear walls. The capacity design concept has been also successfully implemented on RM construction and existence of reinforcement has proved to considerably improve seismic response of masonry construction in terms ductility and energy dissipation (Noland, 1987; Shing et al., 1989, 1990; Abrams and Paulson, 1991; Seible et al., 1994; Tomažević and Weiss, 1994). More recently, there have been further investigations to quantify the seismic performance of RM walls using displacement-based approaches that are more suited towards performance-based design of structures (Shedid et al., 2010a, b; Banting and El-Dakhkhni, 2012, 2014; Shedid and El-Dakhkhni, 2014).

This study presents shake table test results performed on two story RM concrete block walls with design parameters that categorize them as *conventional* (non-seismic) *construction* based on the National Building Code of Canada (NRCC, 2010). The test results are used for realistic quantification of seismic performance of tested walls. A simple analytical model is then calibrated based on the test results and used to predict the seismic response of the tested walls. Finally, analytical fragility curves are generated for the class of the tested walls using the experimental test results and the analytical model. This study is a step forward in better seismic performance quantification of conventional RM construction and evaluation of its seismic risk in Canada.

2. Experimental Program

2.1. Wall Design and Construction

The current paper discusses the test and analysis results of four scaled RM walls, referred to as walls A, B, C, and D hereafter. These four third scale two-story wall specimens were constructed based on dynamic similitude requirements (Harris and Sabnis, 1999). The designs of the walls were selected such that the walls were considered as conventional (non-seismic) construction based on National Building Code of Canada (NRCC, 2010). Furthermore, adequate horizontal reinforcement was provided to prevent shear failure of the walls. The story height of the third-scale two story wall specimens was 1130 mm. Walls A, B, and D had a length of 598 mm while wall C was 865 mm long. The walls were constructed from third scale concrete masonry units (CMU) with a width of 63 mm and average tested compressive strength of 17.7 MPa ($f'_m = 17.7$ MPa). The walls were reinforced with W1.7, D4, and D7 bars with tested yield strength of 281, 490, and 487 MPa, and diameters of 3.8, 5.75, and 7.6 mm, respectively. While the horizontal reinforcements of all of the walls were similar (W1.7@ 130 mm), their vertical reinforcement diameter and spacing were different. Walls A, B, and C had D4 bars spaced at 266 mm, 532 mm, and 399 mm, respectively, while Wall D was reinforced with 2-D7 bars spaced at 532 mm. Fig. 1 shows the elevation of Wall C. More details on the construction of the walls are presented in Mojiri et al. (2015a).

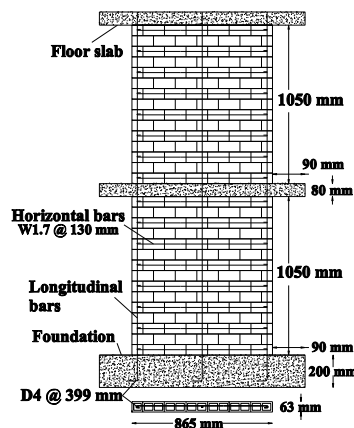


Fig. 1 – Elevation of Wall C

2.2. Test setup and Instrumentation

The model walls were tested under simulated earthquakes using a shake table. A special steel frame was designed and constructed to support majority of the simulated inertial masses of the walls outside the shake table. The frame allowed free unidirectional horizontal movement of the masses with minimal friction. The inertial lateral loads were transferred to the wall specimens through loading beams. This frame was intended to enhance the performance of the shake table and facilitate decoupling of the magnitude of inertial and gravity loads acting on the specimen due to presence of simulated masses. The frame also provided lateral out-of-plane constraint at each story level simulating the rigid in-plane action of the concrete slabs in the prototype building. In order to simulate the axial loads on the wall specimens, the walls were posttensioned on the top floor by two threaded rods connected in series to a soft spring which helped in controlling the increase of the posttensioning axial load due to floor lateral movements. The total inertial mass of walls A, B, and D were 1,097 and 1,119 kg, respectively, for the first and second floors. The total inertial mass was 1158 and 1162 kg, respectively, for the first and second story of Wall C. The total axial stress at the base of the walls was 2% of the compressive strength of masonry ($0.02f_m'$).

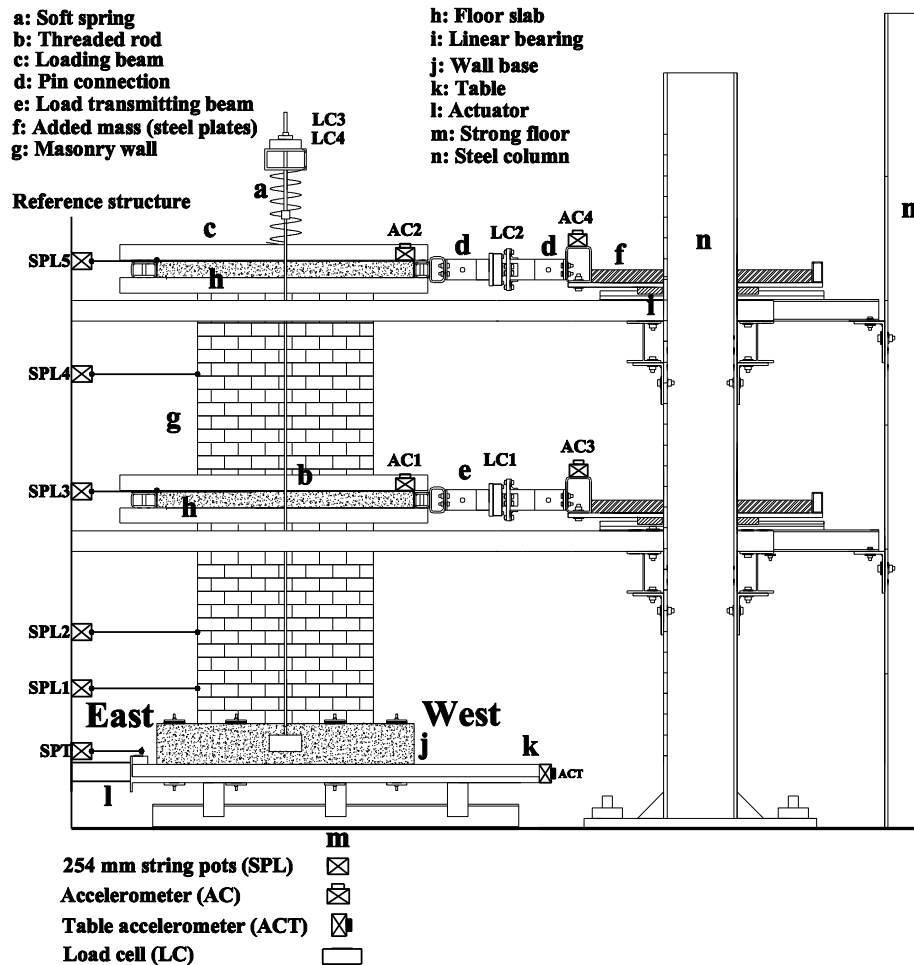


Fig. 2 – Test setup and instrumentation

The test setup was instrumented both internally and externally to measure floor sliding, floor lateral displacements and accelerations, vertical deformations of the walls along their heights and the diagonal deformations in the first story, inertial and axial loads, and the level of strain in the vertical steel reinforcement. Fig. 2 shows an overview of the test setup and some of the external instrumentation. More details about the test setup and instrumentation are presented in Mojiri et al. (2015a).

2.3. Dynamic Excitation

The Loma Prieta 1989 earthquake record at Gilroy Array #2 station was selected from PEER NGA strong motion data base (PEER, 2011). The original record was then scaled to four intensity levels, L0, L1, L2, and L3 with peak ground acceleration (PGA) of 0.19g, 0.24g, 0.61g, and 0.84g covering different seismic hazard levels of high seismic zones in Canada (NRCC, 2010).

3. Analysis of Test Results

3.1. Overview of Experimental Results

The measured response of the tested walls indicated that the failure modes of the walls were in the form of steel yielding followed by crushing of the masonry and subsequent buckling and failure of the vertical bars located at the wall toes that is representative of flexural response. The major crack patterns in the walls were horizontal cracks in the wall/base interface and vertical cracks in the wall toe regions resulting from flexural response of the walls. The shear cracks were limited to horizontal sliding cracks along the wall/base interface. Yielding of the vertical bars occurred for all of the walls during the tests. Both vertical end bars failed after buckling in Walls A, B, and C at either the L2 or L3 level tests. However, in Wall D, only one of the vertical bars failed at the L3 level. Failure of vertical bars was followed by extensive base sliding and rocking of the walls resulting in further damage to the wall toes. However, the overall integrity of all of the walls was maintained even after the highest intensity tests.

The relative lateral displacement, drift ratio, and acceleration response histories at the top of Wall A for test levels L1, L2, and L3 are presented in Fig. 3. The results show that the maximum top drift ratio of Wall A during L1, L2, and L3 test levels is 0.5, 2.3, and 4.5%, respectively. The low frequency cyclic response both in displacement and acceleration response history that is mainly observed during L3 level test is attributed to buckling and failure of both end vertical bars and subsequent loss of strength and extensive rocking of the wall. Fig. 4 shows the moment-curvature hysteresis of Wall A during L1 and L2 level tests. The results indicate extensive nonlinear response and energy dissipation in the wall during L2 level test. Similar responses are observed for walls B, C, and D. More detailed analyses of the energy dissipation mechanisms and capacity of the walls are presented in Mojiri et al. (2014).

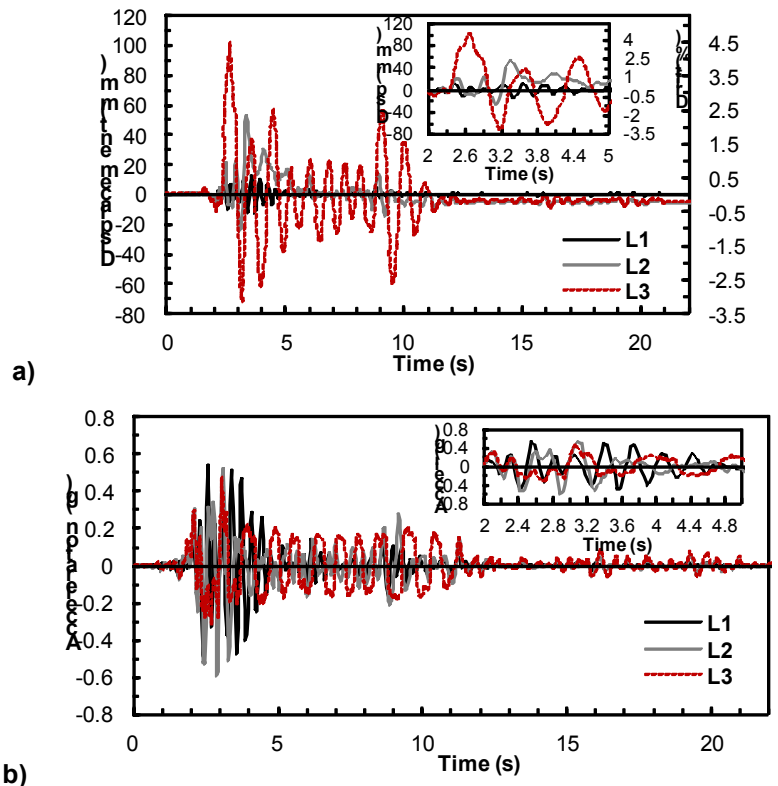


Fig. 3 – Top floor response history of Wall A: a) relative displacement; b) absolute acceleration

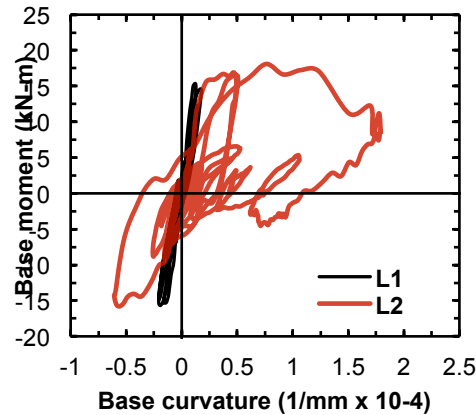


Fig. 4 – Base moment-curvature hysteresis of Wall A during L1 and L2 level tests

3.2. Analysis of Nonlinear Deformations

The values of displacement ductility of the walls are calculated based on shake table test results as a measure of nonlinear response and capacity of the tested walls. The values of displacement ductility are calculated as the ratio of the top floor displacement at maximum lateral load attained by the walls during the tests, referred to as the nominal strength, and the yield displacement of the walls. The yield displacements of the walls are calculated based on the approach suggested by Priestly et al. (2007) as the point of intersection of the line connecting the origin to the point of the experimental yield and corresponding displacement, and extending up to the level of the nominal strength. The experimental yield load in this case is defined as the onset of yielding of the wall end vertical bars. The values of displacement ductility of the walls calculated based on the above approach are 4.6, 2.7, 4.2, and 3.3 for walls A, B, C, and D, respectively. Following an equal-displacement approach (NRCC, 2010), the values of ductility related seismic response modification factors (R_d) which are used in force-based seismic design of structures in many modern seismic design codes including NBCC (NRCC, 2010) will be equal to the displacement ductility values and thus will be in the range of 2.7-4.6. It should be noted that these values are obtained for the walls that are not even permitted as SFRS in seismic zones based on NBCC (NRCC, 2010) due to their reinforcement scheme. Furthermore, in contrary to many modern seismic design codes that prescribe a single value of R_d for each SFRS category, the test results suggest a range of R_d values for this type of walls.

Fig. 5 shows the average curvature profile for Wall A along its height normalized to the experimental yield curvature at the base of the wall. The curvature values are computed based on the masonry compressive and steel tensile strains directly measured during the tests at each wall end at the experimental yield level and top floor drift ratio of 0.5 and 1%. Fig. 5 indicates development and concentration of nonlinear deformations close to the base of the walls, in a plastic hinge region, similar to RC shear walls. The curvature profiles of other tested walls also show similar trend. The equivalent plastic hinge length of the walls are calculated assuming constant plastic curvature in the plastic hinge region and rigid body rotation of the walls around the center of this region (Paulay and Priestly 1992). The equivalent plastic hinge lengths of walls A, B, C, and D obtained following the above approach and calculated at top floor drift ratio of 1% are 122, 100, 102, and 107 mm, respectively which is in the range of 12-20% of the length of the walls. It should be noted that while the test results indicate development of plastic hinge region at the base of the walls, since the tested walls are not permitted as SFRS in seismic zones by NBCC (NRCC, 2010), no specific plastic hinge value is provided in CSA S304.1 (CSA, 2004) for this wall category. Further details about the calculation of equivalent plastic hinge length and displacement and curvature ductility of the walls are presented in Mojiri et al. (2014, 2015a).

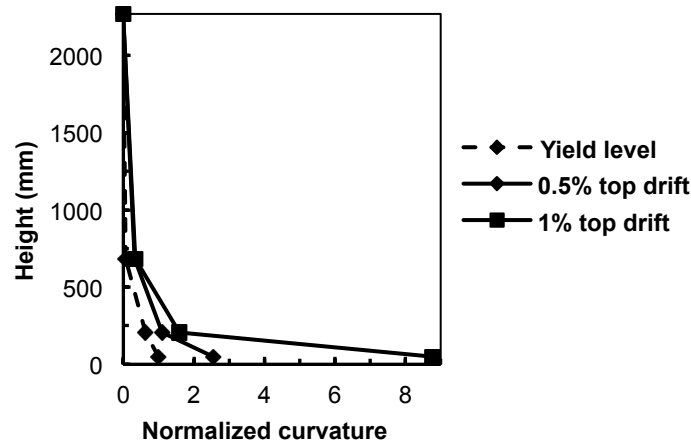


Fig. 5 – Normalized average curvature profile for Wall A

4. Analytical Modeling

4.1. Model Characteristics and Calibration

A simple analytical model was used to predict the response of the tested walls. For this purpose, a two-dimensional beam element with lumped plasticity model was used to model the walls at each story. In this model, the nonlinear behaviour is concentrated at the plastic hinge regions located at the element ends and the rest of the element behaves in linear elastic manner. This model is suitable for response prediction of structural elements with dominating flexural response like the tested walls. While linear elastic response was assumed for the diagonal shear behaviour of the walls, the sliding shear response was neglected. This was consistent with the experimental observations and analysis results that indicated minor contribution of sliding shear deformations to the overall response of the walls (see Mojiri et al., 2015a). A Fukada trilinear moment-curvature hysteretic model with degrading stiffness (Fukada, 1969) was used to model the nonlinear behaviour of the plastic hinge regions. In this model the change in the stiffness due to cracking of the wall prior to yielding is implemented. This model is also capable of modeling the stiffness degradation of the walls. The model parameters are the flexural stiffness of the first segment of the hysteresis (K_0), ratio of pre-yield flexural stiffness to initial elastic flexural stiffness (α), ratio of post-yield flexural stiffness to initial elastic flexural stiffness (r), and the cracking and yield moments (M_{cr} and M_y). In order to model the flexural failure of the walls, a flexural strength degradation model was used based on the maximum curvature ductility of the walls. In order to simulate the energy dissipation of the system through the coulomb friction in the test setup including the mass supporting system, nonlinear springs with elastic-perfect plastic hysteresis were used at each floor level in the model.

NRHA was performed on the wall models using the Ruaumoko code (Carr 2004) with P-delta effects enabled. The parameters of the analytical model were calibrated based on the experimental results presented in the previous sections. Between others, the initial elastic stiffness of the walls (K_0) was calibrated using the results of static pull-back tests that was performed on the walls prior and after each shake table test. Furthermore, in order to calibrate the Fukada hysteresis model, the wall yield moments were evaluated at the onset of yielding of the end vertical bars and the cracking moments were assumed one-third of the yielding moments. Elastic viscous damping of 1% was used for each mode in the models. This value resulted in the best match between the analytical predictions and experimental values. More details about calibration of other parameters are presented in Mojiri et al. (2015b).

4.2. Analysis Results

The elastic periods of the walls were predicted analytically and were compared with the experimentally obtained elastic periods that were calculated from static pull-back tests. The comparison shows an average error of 6.25 % for walls A, B, C, and D. Fig. 6 compares the experimental and analytical base shear response history and base moment-curvature hysteresis response of Wall C. The results indicate

that there is a good agreement between the experimental results and analytical predictions. Similar agreements are observed for other types of response and for other tested walls. The deviations in all cases can be mainly attributed to the inherent approximations in the simplified plastic hinge hysteresis model used in the plastic hinge region and design characteristics that were not considered in the model affecting the flexural response of the walls. Overall, considering the complex nature of RM, the analytical models suggest an acceptable level of accuracy.

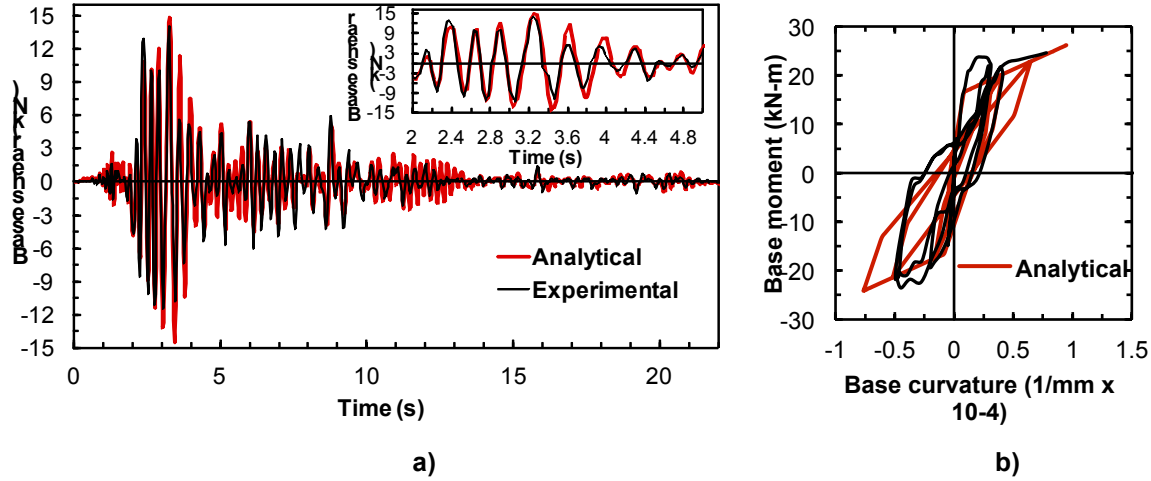


Fig. 6 – Comparison of experimental and analytical responses of Wall C: a) base shear response history; b) base moment-curvature hysteresis

5. Fragility Assessment

Fragility assessment of a structural component or SFRS requires identification of relevant and practical limit states, determination of capacity of the structural component or SFRS for those limit states, and finally measurement, estimation, or prediction of response of the structural component or SFRS under several ground motions with varying intensity. Given the above information, the fragility curves of a structural component or SFRS for a limit state can be obtained as the conditional probability that the seismic demand (D) on the structural component or SFRS exceeds the capacity when an earthquake with certain intensity occurs. This statement can be mathematically expressed by the following equation (Melchers, 2001):

$$P[D > C | IM] = \Phi \left[\frac{\ln(S_d/S_c)}{\sqrt{\beta_{d|IM}^2 + \beta_c^2}} \right] \quad (1)$$

In the above equation S_c and β_c are the median and dispersion of the capacity, S_d is the median of the demand, and $\beta_{d|IM}$ is the dispersion of the demand for a given intensity level represented by an intensity measure (IM). In Eq. 1, Φ is the standard normal Cumulative Distribution Function (CDF). The main assumption in Eq. 1 is that both demand and capacity follow a lognormal probability distribution (Wen et al., 2003).

5.1. Limit States and Wall Capacities

The limit states defined for fragility analysis should have direct relationship with damage levels that have known qualitative and operational implications. Table 1 shows the different limit states considered in this study and their quantitative and qualitative identifications defined based on the shake table test results on the walls. The capacities of the tested walls in terms of top floor drift ratio for each limit state are also obtained based on the shake table test results. The results show a median capacity (S_d) of 0.07, 0.26, and 1.24% and a dispersion (β_c) of 0.44, 0.42, and 0.33 for LS1, LS2, and LS3 limit states, respectively. Since only a limited number of wall specimens were tested and all possible configurations that exist in a

real masonry building are not taken into account during the tests, the square root of sum of squares of each dispersion value and an added dispersion value of 0.25 is considered as the final dispersion of the capacity of the tested walls following the FEMA P-58 (ATC, 2012) recommendations. The final dispersion values are 0.51, 0.49, and 0.41 for LS1, LS2, and LS3 limit states, respectively.

Table 1 – Definition of limit states and their qualitative and quantitative identification.

Limit State	Qualitative Identification	Quantitative Identification
LS1	Minor damage to the wall, minimal horizontal cracking along mortar lines affecting surface finishes	Cracking base moment (M_{cr})
LS2	Moderate damage to the wall, limited cracks in the face shells, horizontal cracks along mortar lines and at the base of the wall	Yield base moment (M_y)
LS3	Severe cracks in the wall toe region face shells, wide horizontal cracks along the mortar lines and at the base of the walls, extensive yielding of the reinforcement bars, permanent wall deformations	Ultimate moment capacity (M_u)

5.2. Seismic Demands

Probabilistic Seismic Demand Analysis (PSDA) was performed following the approach suggested by Cornell et al. (2002). In this approach the models are tested under several earthquakes with varying intensity and the maximum demands (D) during each earthquake are plotted against the Intensity Measure (IM). Assuming that S_d is related to IM with $S_d = A(IM)^B$, a regression is performed to find parameters A and B and the equation for the median of demand is derived in terms of IM . The $D - IM$ data points and S_d are then used to calculate $\beta_{d|IM}$. In the absence of a large experimental data base required to quantify the wall analytical model uncertainties, the dispersion of the demands resulting from uncertainties in the wall analytical models is not considered in this study. Furthermore, in order to reduce the dependency of the structural response on the selected ground motions and thus reduce the demand dispersion, the spectral acceleration at the elastic fundamental period of the walls ($S_a(T)$) is chosen as the intensity measure in this study.

To determine the demands, 30 synthetic ground motions compatible with NBCC (NRCC, 2010) uniform hazard spectra with 2% chance of exceedence in 50 years were selected from the data base developed by Atkinson (2009). The selected records had varying fault distance, magnitude, and soil conditions and were located in both western and eastern areas of Canada. The records were grouped in five ranges of spectral acceleration bins. 120 NRHA were performed on the scaled wall models to determine the $D - IM$ data points. The results are indicated in Fig. 7-a. This figure also shows the linear least squares regression results. The calculated values for $\beta_{d|IM}$ is 0.4.

5.3. Generation of Fragility Curves

Following the calculation of all the required parameters in Eq. 1, the fragility curves for the tested walls and the defined limit states are generated and presented in Fig. 7-b. The average design spectral acceleration over the wall periods for some of the cities of Canada with different levels of seismicity as specified by the NBCC (NRCC, 2010) are also shown in this figure. The fragility curves provide valuable information on the seismic risk evaluation of conventional RM in Canada. Based on these curves, in the city of Montreal, which is one of the seismic regions in Canada, although there is a very high chance that the walls exceed LS1 limit state affecting the surface finishing and causing minor damage, there is almost no chance that the walls exceed limit state LS3, causing extensive level of damage that requires major wall repair. It can also be inferred that even for the cities of Vancouver and Victoria and for the islands of Haida Gwaii, which are in the highest seismic regions of Canada, there is only 5, 16, and 30% chances, respectively, that the walls will exceed the LS3 limit state. The above observations confirm the effectiveness of inclusion of light amount of reinforcement on increasing the seismic performance of the lightly reinforced masonry walls and the potential capacity of these walls to resist seismic lateral loads

even in highest seismic regions of Canada. The fragility curves developed for the walls can be extrapolated to RM buildings (system level) assuming modular symmetrical RM construction and ignoring the possible coupling between the walls; thus resulting in similar dynamic characteristics of the individual walls and the building system as a whole.

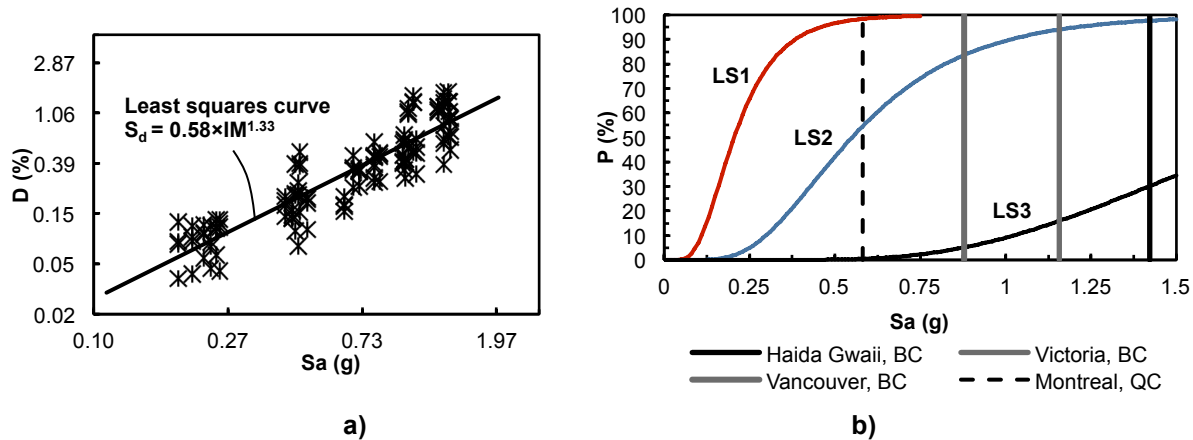


Fig. 7 – Comparison of experimental and analytical responses of Wall C. a) Base shear response history, b) Base moment-curvature hysteresis

6. Conclusions

As a step toward quantification of seismic performance and risk for conventional RM construction, the results of recent shake table tests on lightly RM walls were evaluated and discussed in this paper. The results indicated that even minor inclusion of steel reinforcement in masonry walls significantly increases the ductility and energy dissipation characteristics of the walls. The walls mainly responded and failed in flexure and rendered controllable and predictable lateral response. In general, the walls experienced minimal damage under low amplitude shaking corresponding to frequent minor earthquake events, incurred repairable damage for higher level tests, and maintained their integrity for the highest level tests corresponding to the highest seismicity zones in Canada. Based on the test results, the walls were able to form plastic hinging mechanism at their base and dissipate energy there. The observed seismic performance of the tested walls were well above what is currently recognized for the class of RM construction tested. It was further indicated that the response of the walls can be well predicted by a simple and calibrated analytical model. The experimental results and the analytical model then were used to produce fragility curves for the tested walls for a range of earthquakes with varying intensity. The fragility curves indicated that for walls with design parameters similar to the ones considered in this study, there is a maximum of 30% chance that two-story, lightly reinforced masonry shear walls would undergo extensive damage requiring significant repairs even in some of the highest seismic zones of Canada. These observations indicate that currently perceived seismic performance capabilities of these lightly RM SFRS may be underestimated by the Canadian standards (CSA, 2004; NRCC, 2010) which do not permit these types of construction in regions of moderate seismicity.

7. References

- Applied Technology Council (ATC). *Interim Testing Protocols for Determining the Seismic Performance Characteristics of Structural and Nonstructural Components (FEMA-461)*. Applied Technology Council. Federal Emergency Management Agency, Washington D.C., USA, 2007.
- Applied Technology Council (ATC). *Next-generation Methodology for Seismic Performance Assessment of Buildings, (FEMA P-58)*. Applied Technology Council. Federal Emergency Management Agency, Washington D.C., USA, 2012.
- Atkinson, G. M. "Earthquake Time Histories Compatible with the 2005 National Building code of Canada Uniform Hazard Spectrum." *Canadian Journal of Civil Engineering*, 36(6), 991–1000, 2009.
- Banting, B. and El-Dakhkhni, W. "Force- and Displacement-Based Seismic Performance Parameters for Reinforced Masonry Structural Walls with Boundary Elements." *Journal of Structural Engineering*, 138(12), 1477–1491, 2012.
- Banting, B. and El-Dakhkhni, W. "Seismic Performance Quantification of Reinforced Masonry Structural Walls with Boundary Elements." *Journal of Structural Engineering*, 140(5), 04014001, 2014.
- Carr, A. J. *Ruaumoko, Volume 1: Theory Manual*, Dept. of Civil Engineering, Univ. of Canterbury, Christchurch, New Zealand, 2004.
- Canadian Standard Association (CSA). *Design of Masonry Structures*, CSA S304.1, Mississauga, ON, 2004.
- Cornell, C., Jalayer, F., Hamburger, R., and Foutch, D. "Probabilistic Basis for 2000 SAC Federal Emergency Management Agency Steel Moment Frame Guidelines." *Journal of Structural Engineering*, 128, SPECIAL ISSUE: STEEL MOMENT FRAMES AFTER NORTHRIDGE—PART II, 526–533, 2002.
- Drysdale, R., and Hamid, A. *Masonry Structures: Behavior and Design*. 3rd Ed., Canada Masonry Design Centre, Mississauga, Canada, 2005.
- Fukada, Y. "Study on the Restoring Force Characteristics of Reinforced Concrete Buildings." *Proceedings of Kanto District Symposium*, Architectural Institute of Japan, Tokyo, Japan (in Japanese), 1969.
- Harris, H. G., and Sabnis, G. *Structural Modeling and Experimental Techniques*. 2nd Ed., CRC Press, Boca Raton, FL, 1999.
- Melchers, R. E. *Structural Reliability Analysis and Prediction*, 2nd Ed., Wiley, West Sussex, England, 2001.
- Mojiri, S., Tait, M., and El-Dakhkhni, W. "Seismic Response Analysis of Lightly Reinforced Concrete Block Masonry Shear Walls Based on Shake Table Tests." *Journal of Structural Engineering*, 140(9), 04014057, 2014
- Mojiri, S., El-Dakhkhni, W., and Tait, M. "Shake Table Seismic Performance Assessment of Lightly Reinforced Concrete Block Shear Walls." *Journal of Structural Engineering*, 141(2), 04014105, 2015a.
- Mojiri, S., El-Dakhkhni, W., and Tait, M. "Seismic Fragility Evaluation of Lightly Reinforced Concrete-Block Shear Walls for Probabilistic Risk Assessment." *Journal of Structural Engineering*, 141(4), 04014116, 2015b.
- National Research Council of Canada (NRCC). *National Building Code of Canada (NBCC)*. Institute for Research in Construction, Ottawa, Canada, 2010.
- Nielson, B. G. *Analytical fragility curves for highway bridges in moderate seismic zones*. Ph.D. thesis, School of Civil and Environmental Engineering, Georgia Institute of Technology, Atlanta, GA, 2005.
- Pacific Earthquake Engineering Research Center (PEER). NGA Database. (<http://www.peer.berkeley.edu/nga/>), September 2011.
- Paulay, T., and Priestley, M. J. N. *Seismic Design of Reinforced Concrete and Masonry Buildings*, Wiley, New York and Toronto, 1992.

Priestley, M. J. N., Calvi, G. M., and Kowalsky, M. J. *Displacement-Based Seismic Design of Structures*, Istituto Universitario di Studi Superiori di Pavia (IUSS), Pavia, Italy, 2007.

Shedid, M., El-Dakhakhni, W., and Drysdale, R. "Seismic Performance Parameters for Reinforced Concrete-Block Shear Wall Construction." *Journal of Performance of Constructed Facilities*, 24(1), 4–18, 2010a.

Shedid, M., El-Dakhakhni, W., and Drysdale, R. "Alternative Strategies to Enhance the Seismic Performance of Reinforced Concrete-Block Shear Wall Systems." *Journal of Structural Engineering*, 136(6), 676–689, 2010b.

Shedid, M. and El-Dakhakhni, W. "Plastic Hinge Model and Displacement-Based Seismic Design Parameter Quantifications for Reinforced Concrete Block Structural Walls." *Journal of Structural Engineering*, 140(4), 04013090, 2014.

Shome, N. *Probabilistic Seismic Demand Analysis of Nonlinear Structures*. Ph.D. thesis, Dept. of Civil and Environmental Engineering, Stanford University, Redwood City, CA, 1999.

Wen, Y. K., Ellingwood, B. R., Veneziano, D., and Bracci, J. *Uncertainty Modeling in Earthquake Engineering*. FD-2 Rep. 12, Mid-America Earthquake (MAE) Center, Urbana, IL, 2003.